Supplementary Information

Multifunctional and Multimodality Theranostic Nanomedicine for Enhanced Phototherapy

Libiao Yan,[#,a] Siqi Lin,[#,a] Lina Wang,[c] Yupeng Wang,*[,a,b] Dongfang Zhou,[a,b] Qingbing Zeng*[,a]

[a] NMPA Key Laboratory for Research and Evaluation of Drug Metabolism, Guangdong Provincial Key Laboratory of New Drug Screening, School of Pharmaceutical Sciences, Southern Medical University, Guangzhou 510515, P. R. China..

[b] Department of Ultrasonic Diagnosis, Zhujiang Hospital, Southern Medical University, Guangzhou 510282, P. R. China.

[c] Testing and Analysis Center, Hebei Normal University, Shijiazhuang, 050024, P. R. China

* Correspondence should be addressed to ypengwang@126.com, zengqb@smu.edu.cn.

[#] These authors contributed equally to this manuscript.

Materials and characterizations

Potassium permanganate, diethyl ether, hydrochloric acid, hydrogen peroxide were purchased from Guangzhou Chemical Reagent Factory. Polyethylene imine, chlorin e6, dopamine hydrochloride, polyethylene imine, 1-ethyl-(3-dimethylaminopropyl) carbonyl diimide, polyethylene imine, trimethylol aminomethane,anhydrous ethanol , sodium hydroxide were purchased from Shanghai Maclin Biochemical Technology Co., LTD. N- hydroxysuccinimide and dimethyl sulfoxide were purchased from Shanghai Aladdin Reagent Co., LTD. 2,7-Dichlorodi -hydrofluorescein diacetate was purchased from Sigma-Aldrich USA. Dulbecco's Modified Eagle's Medium (DMEM) High Sugar Medium, Penicillin-streptomycin solution, Fetal bovine serum (FBS) ,trypsin were purchased from Thermo Fisher, USA. DAPI anti-fluorescence quenching sealing tablet Solution Shanghai Biyuntian Biotechnology Co., LTD.

Thiazole blue was purchased from Beijing Solaibao Technology Co., LTD. Above chemicals of AR grade were used without purification. Malvern Zetasizer Nano ZS was applied to measured dynamic light scattering (DLS) and Zeta potentials.Transmission electron microscopy (TEM) images was taken by FEI Talos F200S electron microscope and scan electron microscopy (SEM) images was taken by Hitachi S4800. Brunner−Emmet−Teller (BET) measurements was performed on ASAP2460 aperture analyzer. The X-ray diffraction was dectected by Bruker D8 advance X-Ray Diffractometer. Ultraviolet absorption spectrum and fluorescence emission spectrum were obtained with UV-5500PC and SHIMADZU RF-6000 respectively. Deionized water used in the experiment was produced by ultra-pure water system (Master touch-RUV, HHitech).

Stability experiments of $HMnO_2$/C&P

The stability of $HMnO_2$/C&P was evaluated in PBS (0.01 M, 37 ℃, pH 7.4) containing 10% FBS. The size distribution of $HMnO_2$/C&P nanoparticles was analyzed daily by DLS for 7 days.

PH-dependent decomposition of $HMnO_2$/C&P

MnO_2 is acid responsive, so TEM was used to investigate the acid responsive effect of $HMnO_2$/C&P. $HMnO_2$/C&P was dissolved in PBS (10 mM H_2O_2, pH 5.7), and sampled at different time points (0 h, 2 h and 6 h) and added to copper net for sample preparation. Finally, the morphologies were observed by TEM.

Live and dead staing

HepG2 cells were planted in 6-well plates. When the growth density reached 80% of the maximum density, DMEM containing $HMnO_2$/C&P was added for 12-hour incubation. The cells were irradiated with 808 nm laser (1 W·cm^2, 10 min), 660 nm laser (100 mW·cm^2, 30 s) and 808 nm laser (1 W·cm^2, 10 min) + 660 nm laser (100 mW·cm^2, 30 s), respectively. Dissolving in serum-free DMEM medium, 500 μL of Calcein-AM/PI solution was added to each well, and incubated for 30 min. Then the cells were washed with PBS twice and observed via fluorescence microscope.

***In vivo* fluorescence imaging**

$HMnO_2$/C&P was dissolved in PBS and was injected intravenously into tumor-bearing Kunming mice (300 μg Ce6 mL^{-1}, 3 mg Ce6 kg^{-1}). The fluorescence of Ce6 distribution was observed by fluorescence imaging system for animals at 6 h, 12 h and 24 h, respectively.

Infrared thermal image

The infrared thermal imaging camera was used to measure the temperature of tumor under 808 nm laser. A tumor bearing Kunming mouse was observed by an infrared thermal imaging camera under 808 nm laser without injection. $HMnO_2$/C&P was administered to the mouse intravenously. 12 hours later, the infrared camera was applied to monitor the temperature of tumor site under 808 nm laser.

Intratumoral infrared thermography of $HMnO_2$/C&P

Kunming mice were injected with PBS and $HMnO_2$/C&P solution through the tail vein, and the tumor site was irradiated with 808 nm laser for 5 min after 6 h. Infrared thermal imager was used for observation during irradiation. The tumor site was imaged and temperature recorded every minute.

Photothermal Conversion Efficiency of $HMnO_2$/C&P

Photothermal conversion efficiency of the $HMnO_2$/C&P was calculated according to a reported method. First, the $HMnO_2$/C&P (200 mg/mL) in solution were irradiated with 808 nm laser (1 W/cm^2) for 450 s and then the laser was turned off. After about 600 s, the temperature of the solution was cooled to room temperature. The photothermal conversion efficiency (η) was calculated according to the following equation

$$\eta = hA\,(\Delta T_{max,\,mix} - Q_s)/\,I(1 - 10^{-A808}) \times 100\% \qquad (1)$$

Here h is the heat transfer coefficient, A is the surface area of the container, and T_{max} and T_{mix} represent the maximum temperature and the room temperature of the environment. Qs is how much heat a solvent absorbs light per second. I is the laser power. A808 is the absorbance of $HMnO_2$/C&P at 808 nm, and η is the conversion efficiency. hA can be determined by applying the linear time data from the cooling

period vs –lnθ. τ_s works out to be 273.14s.

$$hA = m C_p / \tau_s \quad (2)$$

where m(2×10^{-3} Kg) and Cp are the mass and heat capacity of solvent (water), respectively.

A dimensionless parameter θ was calculated as followed:

$$\theta = (T - T_{sur})/(T_{max} - T_{Sur}) \quad (3)$$

A sample system time constant τ_s could be calculated as followed:

$$t = -\tau_s \ln(\theta) \quad (4)$$

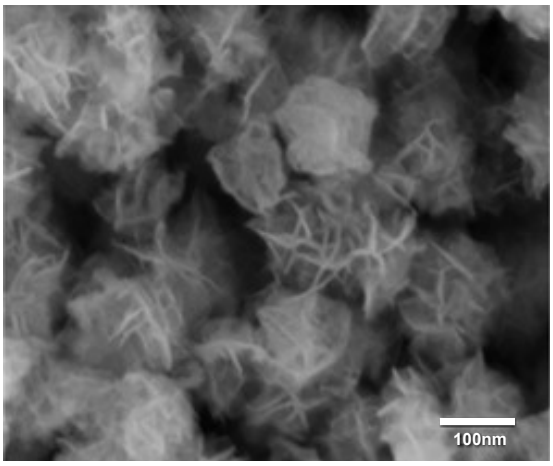

Fig. S1. SEM image of $HMnO_2$ nanoparticles (scar bar=100 nm).

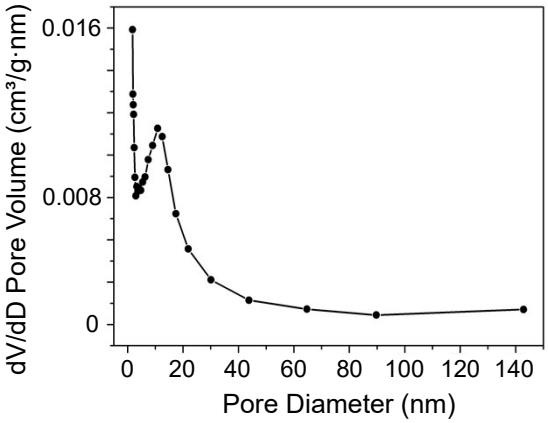

Fig. S2. Pore volume distribution of $HMnO_2$ nanoparticles.

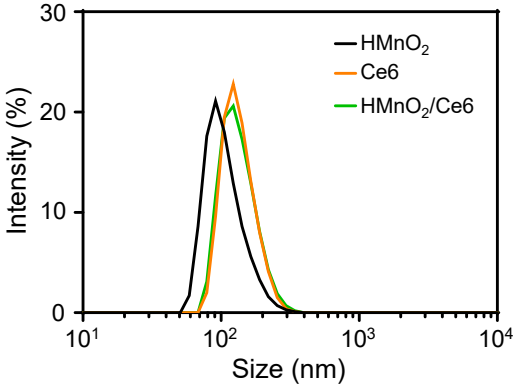

Fig. S3. Particle size distribution of $HMnO_2$, $HMnO_2$-NH_2, $HMnO_2$/Ce6.

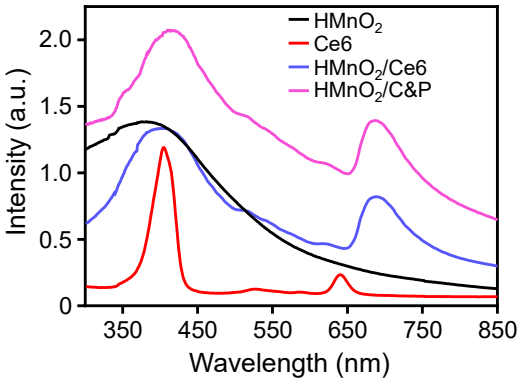

Fig. S4. UV-vis spectrum of $HMnO_2$, Ce6, $HMnO_2$/Ce6, $HMnO_2$/C&P.

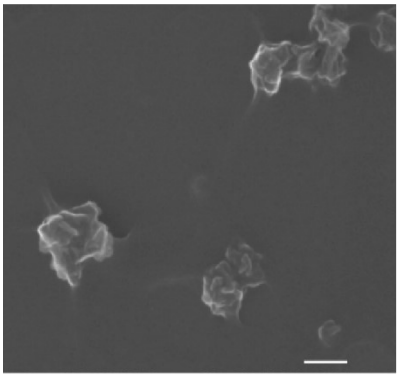

Fig. S5. SEM image of $HMnO_2$/C&P (scale bar=100 nm).

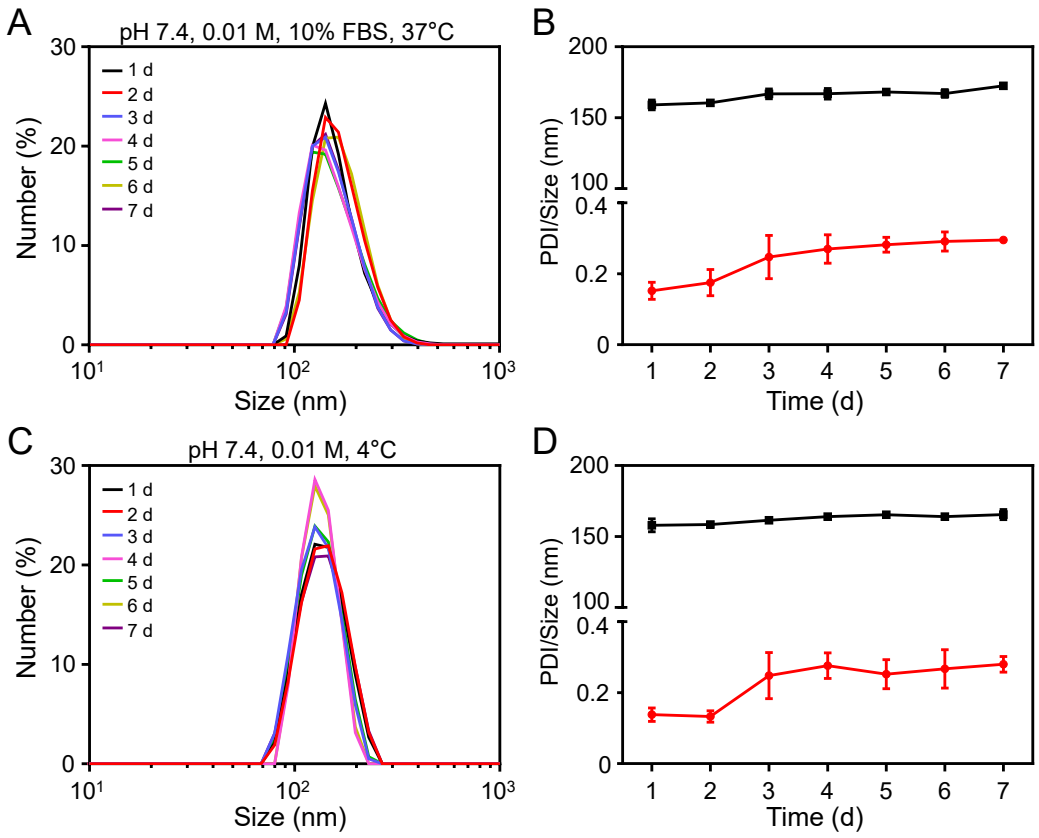

Fig. S6. Particle size stability of $HMnO_2$/C&P in (A, B) PBS 7.4, 37 ℃ (0.01M, 10% FBS), and (C, D) PBS 7.4, 4 ℃ (0.01M).

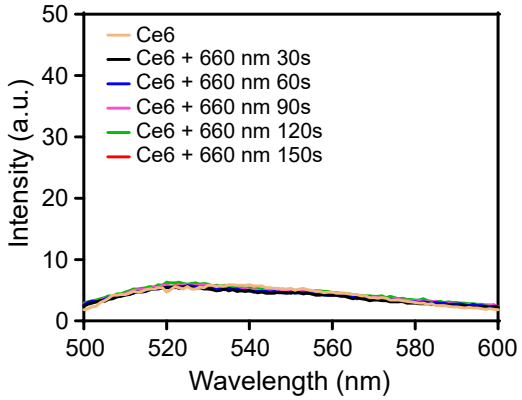

Fig. S7. Fluorescence spectra of DCFH irradiated by 660 nm laser in PBS containing GSH (10 mM) and Ce6.

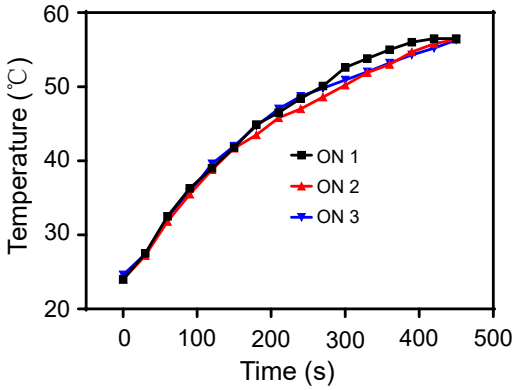

Fig. S8. Temperature rise curve of $HMnO_2$/C&P during three 808 nm laser on-state.

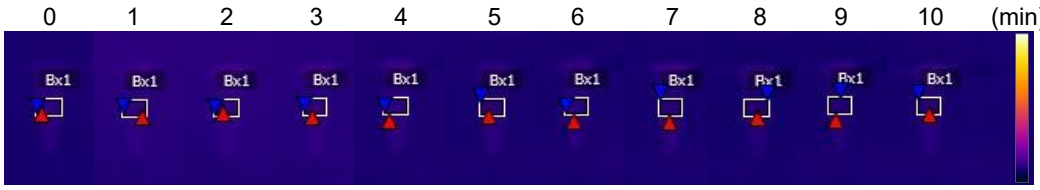

Fig. S9. Infrared thermal images of PBS 7.4 under 808 nm laser irradiation with a power density of 1W/cm^2.

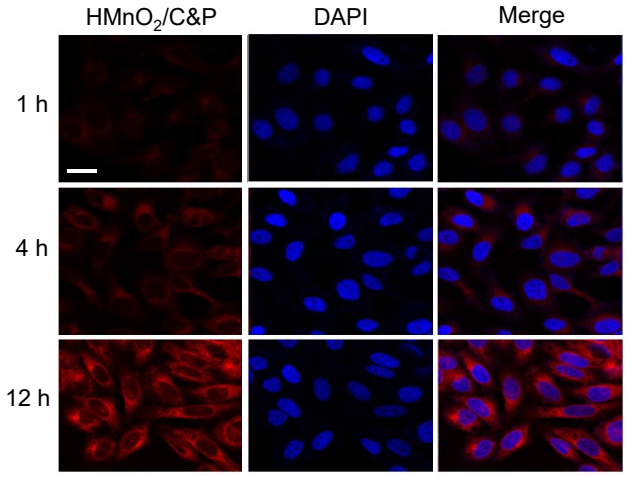

Fig. S10. Confocal fluorescence images of HepG2 cells incubated with $HMnO_2$/C&P for different time (scale bar = 10 μm).

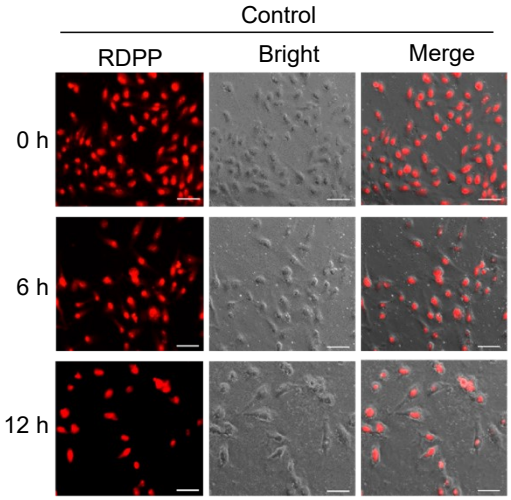

Fig. S11. Intracellular O_2 level detected by oxygen probe RDPP probe (scale bar = 50 μm).

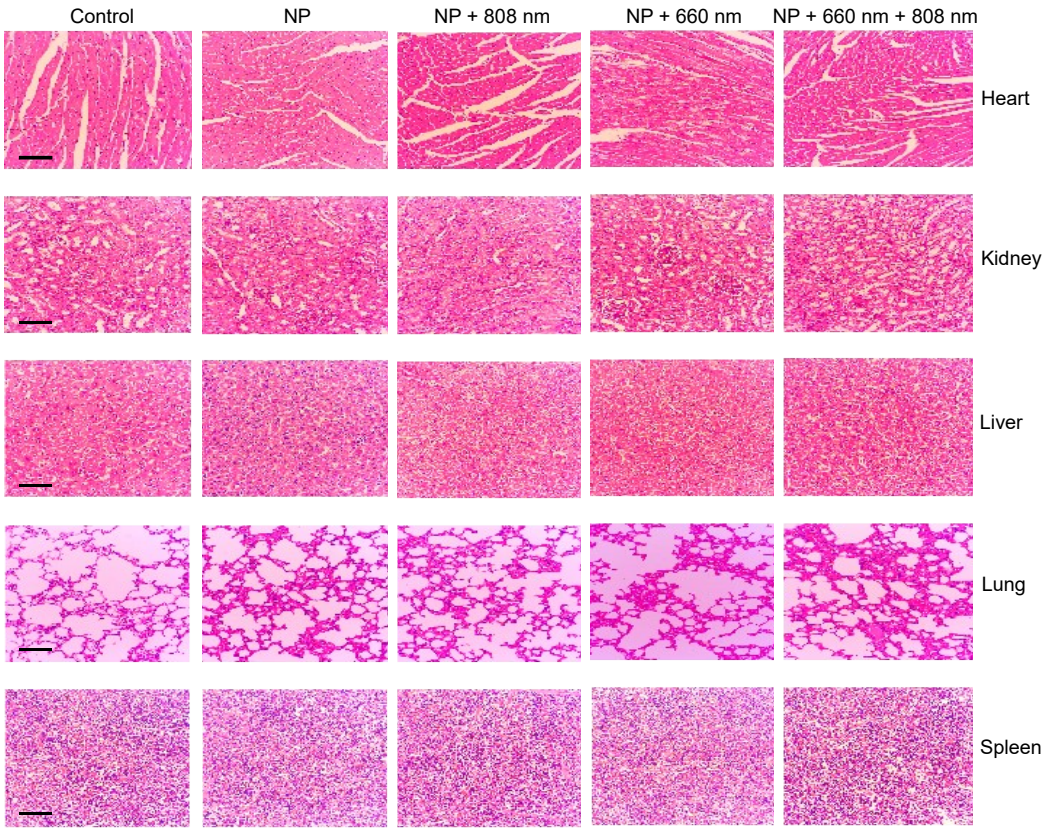

Fig. S12. H&E staining of heart, kidney, liver, lung and spleen (scale bar = 100 μm).